Front. Environ. Sci. Eng. 2023, 17(6): 70
https://doi.org/10.1007/s11783-023-1670-8

RESEARCH ARTICLE

Distribution, enrichment mechanism and risk assessment for fluoride in groundwater: a case study of Mihe-Weihe River Basin, China

Xingyue Qu[1], Peihe Zhai (✉)[1], Longqing Shi[1], Xingwei Qu[2], Ahmer Bilal[1], Jin Han[3], Xiaoge Yu[4]

1 College of Earth Science and Engineering, Shandong University of Science and Technology, Qingdao 266590, China
2 College of Safety and Environmental Engineering, Shandong University of Science and Technology, Qingdao 266590, China
3 College of Computer Science and Engineering, Shandong University of Science and Technology, Qingdao 266590, China
4 Department of Resource and Civil Engineering, Shandong University of Science and Technology, Tai'an 271019, China

HIGHLIGHTS

- High fluorine is mainly $HCO_3 \cdot Cl$-Na and HCO_3-Na type.
- F^- decreases with the increase of depth to water table.
- High fluoride is mainly affected by fluorine-containing minerals and weak alkaline.
- Fluorine pollution is mainly in the north near Laizhou Bay (wet season > dry season).
- Groundwater samples have a high F^- health risk (children > adults).

GRAPHIC ABSTRACT

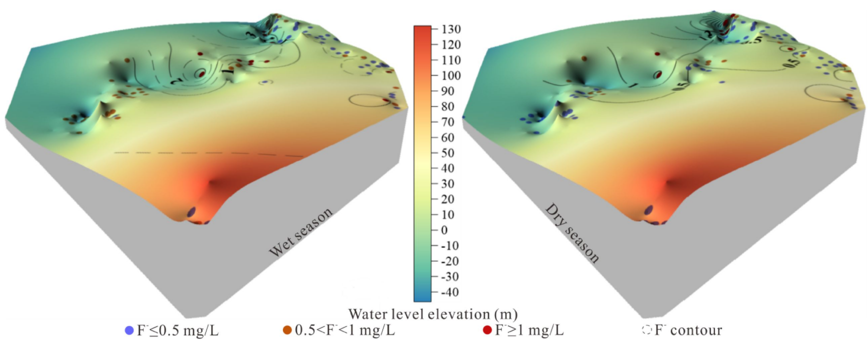

ARTICLE INFO

Article history:
Received 28 June 2022
Revised 12 November 2022
Accepted 15 November 2022
Available online 29 December 2022

Keywords:
Groundwater in the Mihe-Weihe River Basin
Distribution characteristics of fluorine
Factors influencing fluoride
Enrichment mechanism of fluorine
Hydrogeochemical modeling
Pollution and risk assessment

ABSTRACT

Due to the unclear distribution characteristics and causes of fluoride in groundwater of Mihe-Weihe River Basin (China), there is a higher risk for the future development and utilization of groundwater. Therefore, based on the systematic sampling and analysis, the distribution features and enrichment mechanism for fluoride in groundwater were studied by the graphic method, hydrogeochemical modeling, the proportionality factor between conventional ions and factor analysis. The results show that the fluorine content in groundwater is generally on the high side, with a large area of medium-fluorine water (0.5–1.0 mg/L), and high-fluorine water is chiefly in the interfluvial lowlands and alluvial-marine plain, which mainly contains $HCO_3 \cdot Cl$-Na- and HCO_3-Na-type water. The vertical zonation characteristics of the fluorine content decrease with increasing depth to the water table. The high flouride groundwater during the wet season is chiefly controlled by the weathering and dissolution of fluorine-containing minerals, as well as the influence of rock weathering, evaporation and concentration. The weak alkaline environment that is rich in sodium and poor in calcium during the dry season is the main reason for the enrichment of fluorine. Finally, an integrated assessment model is established using rough set theory and an improved matter element extension model, and the level of groundwater pollution caused by fluoride in the Mihe-Weihe River Basin during the wet and dry seasons in the Shandong Peninsula is defined to show the necessity for local management measures to reduce the potential risks caused by groundwater quality.

1 Introduction

Fluorine is one of the essential trace elements for human beings and has a positive effect on metabolism, playing a role in preventing diseases. However, long-term overtaking by fluoride can destroy the enzymes needed for vitamin metabolism; fluoride can not only damage our bones but also lead to the degeneration of brain tissue, the kidney and the central nervous system, which is known

✉ Corresponding author
E-mail: zhaiph2021@163.com

simply as "fluorosis". This is an environmental problem for human health that needs worldwide attention (Kharb and Susheela, 1994; Andezhath et al., 1999; Pillai and Stanley, 2002; Ayoob and Gupta, 2006; Nielsen, 2009; Reddy et al., 2010). Fluorine can go in the humans by potable water, food and air, but the absorption rate in each medium is different. After entering the respiratory tract, almost all fluorine in the air is absorbed, which is harmful to the human body. However, this is a local phenomenon that occurs only in the areas surrounding enterprises that discharge a large amount of fluoride, that is, in the local areas that have severe atmospheric fluorine pollution. Therefore, fluorine in the air can generally be ignored. The fluorine in food has a complex composition and is not easily digested by the human body, so the absorption rate is very low. The fluorine in drinking water can be digested and absorbed by most of the human body, so drinking high-fluorine water is the major cause of "fluorosis". At present, global water resources are facing an extreme shortage, which has caused shallow groundwater to be gradually exploited as a drinking water source in many countries and regions, especially in the arid and semiarid northern regions of China. Currently, greater than 70% of drinking water is supplied by shallow groundwater. Groundwater plays a vital role in supporting the benign development of the ecosystem and maintaining the basic living security of human beings (Jayarathne et al., 2014; Jia et al., 2015; Yin et al., 2021). However, with the rapid growth of industry and agriculture, especially the continuous acceleration of urban construction and the continuous improvement of industrialization, the pollution of shallow groundwater is becoming increasingly severe. In particular, the fluorine content in a large area exceeds the standard, which seriously threatens human health (Qiao et al., 2014; Yu et al., 2018; Zhang et al., 2022). Therefore, clarifying the distribution features and enrichment mechanism for fluorine in groundwater is the basis for solving drinking water problems in fluorosis-prone areas and is also one of the important tasks for treating endemic fluorosis.

Scholars from around the world have performed much work involving the migration and enrichment of fluorine in groundwater. By investigating the distribution of high-fluorine water in India, Jacks et al. (2005) found that high-fluorine groundwater mainly exists in northwestern India and the hard rock area in the southern Ganges valley. Chernet et al. (2001) found that due to the influence of climate, strong evaporation and concentration lead to a continuous increase in the salt concentration and fluorine content in the groundwater of Ethiopia, thus forming high-fluorine water. By monitoring the soil in a forest-covered area in western Switzerland, Egli et al. (2001) found that the aluminum smelting industry in this area will change the chemical properties of the soil, make the fluorine-containing minerals more easily dissolvable, and finally leading to the formation of high-fluorine groundwater in this area. Mooreb and Levya (2004) have studied fluorine and its main chemical elements in the shallow groundwater in the Irvine Lake area in eastern California. Dehbandi et al. (2018) studied the distribution characteristics of fluoride in endemic fluorosis areas in central Iran. Li et al. (2011) found that the dissolution, evaporation and concentration of fluorine-containing minerals are the main factors controlling the fluorine richness in the shallow groundwater of the Taiyuan Basin, China. Lv et al. (2020) found that the fluorine richness in the groundwater of the Qinwangchuan Basin in Gansu Province (China) is mostly affected by the weathering and the dissolution of fluorine-containing minerals in sedimentary strata.

The Mihe-Weihe River Basin is a region with a high fluorine content in the groundwater of Shandong Peninsula in China and is part of the endemic fluorosis area due to long-term overtaking by high-fluorine water. The residents have been severely affected by high-fluorine water for a long time, so it is a key area for the prevention and control of endemic fluorosis in Shandong Province. The standard (GB17018-1997) for the classification of endemic fluorosis is that the fluorine content is greater than 1.0 mg/L, which indicates a low-incidence area; a fluorine content greater than 2.0 mg/L indicates a moderate-incidence area; a fluorine content greater than 4.0 mg/L indicates a severe-incidence area. Based on the investigation of the fluorine content in drinking water, there were 34585 drinking water sources in the basin, and an average of 6–7 households had one well, of which 562 wells were identified as high-fluorine water sources (high incidence area); these wells led to 550000 victims, accounting for 55.9% of the total population; 238 water wells were identified as moderately diseased water sources (medium-incidence area), accounting for 42.35% of the total number of diseased areas. Based on the investigation of endemic fluorosis, 4520 children 8–12 years old and 2002 patients had dental fluorosis, with a prevalence rate of 44.3%. There were 36802 adults over 16 years old and 700 patients with skeletal fluorosis, with a prevalence rate of 1.9%. The enrichment of fluoride in groundwater poses a great threat to the survival of local residents and the sustainable development of the economy. But now there is a lack of research on the migration and enrichment of fluorine in shallow groundwater in the Mihe-Weihe River Basin, as well as the evaluation of environmental quality and human health caused by fluorine pollution. The negative effects of fluorine pollution in shallow groundwater are not clear. To solve the above problems, the work of preventing fluoride and improving groundwater quality in the Mihe-Weihe River Basin has been developed in a scientific and rational direction, and the methods for exploitation, utilization and management, suitable for the local situation, has become an important research content. The results of this paper can not only provide a scientific basis for the sustainable utilization of local groundwater resources and the improvement of the water quality, but have great guiding significance for the treatment of fluorine pollution in local shallow groundwater and the regional environmental planning.

2 Study area

Study area is the Mihe-Weihe River Basin, mainly six rivers, from south to north, the topography from higher to lower is alluvial plain, diluvial plain and marine plain, and the maximum elevation in study area is 1032 m. A sub-humid warm temperate continental monsoon climate, the minimum temperature is in January (mean temperature −3.3 °C), while the maximum in July (mean temperature 26.0 °C). The average annual precipitation is 613.88 mm, and the maximum and minimum precipitation is 948.24 mm and 386.44 mm. The precipitation higher than the average is mainly in the south, while in the north, it is lower than the annual average, and east > west.

Quaternary unconsolidated sediments are widely distributed in the study area, and Paleoproterozoic, Neoproterozoic, Paleozoic, Mesozoic, and Cenozoic strata are exposed. The groundwater in the Mihe-Weihe River Basin is mainly divided into three categories: Quaternary pore water, carbonate karst fissure of water and bedrock fissure water, in which pore water is the main type, mainly in the southern piedmont, and is divided into shallow pore water and deep pore water. Saline water and brackish water are in the northern coastal plain. The coastal areas are basically salty water, a little brine water (Fig. 1).

3 Materials and methods

3.1 Sample collection and testing

Eighty-seven groundwater samples collected in September 2017 (wet season) and ninety-two groundwater samples collected in May 2017 (dry season) were from the same common wells that were in use at the same locations in the Mihe-Weihe River Basin. Two 50 mL polyethylene bottles washed with distilled water were used for filtered groundwater samples in the wet season. One was acidified to pH = 2 for cation measurement, and the other was used for anion measurement without adding reagents. Sampling in the dry season was similar. Two 500 mL polyethylene bottles were used for unfiltered groundwater samples in the wet and dry seasons for alkalinity. The basic parameters (pH, TDS, T and EC) were tested on site and other hydrochemical indexes were tested in the lab.

3.2 Analytical methods

3.2.1 Factor analysis

Step 1: The suitability of the original variables for factor analysis are assessed, and strong correlations between two variables are necessary.

Step 2: The factor variables are constructed (Xue, 2015):

$$\begin{cases} x_1 = a_{11}F_1 + a_{12}F_2 + \cdots + a_{1m}F_m + a_1\varepsilon_1 \\ x_2 = a_{21}F_1 + a_{22}F_2 + \cdots + a_{2m}F_m + a_2\varepsilon_2 \\ \cdots \\ x_p = a_{p1}F_1 + a_{p2}F_2 + \cdots + a_{pm}F_m + a_p\varepsilon_p \end{cases}$$

where $x_1, x_2, \cdots, x_p$ are original variables. $F_1, F_2, \cdots, F_m$ are factor variables. a_{ij} is the factor loading. ε is the specific factor.

Step 3: Rotational methods are adopted to make factor variables more solvable, and original variables ($x_1, x_2, \cdots, x_p$) are converted to uncorrelated variables ($y_1, y_2, \cdots, y_p$) by linear variation (Xue, 2015):

$$\begin{cases} y_1 = \mu_{11}x_1 + \mu_{21}x_2 + \cdots + \mu_{p1}x_p \\ y_2 = \mu_{12}x_1 + \mu_{22}x_2 + \cdots + \mu_{p2}x_p \\ \cdots \\ y_p = \mu_{1p}x_1 + \mu_{2p}x_2 + \cdots + \mu_{pp}x_p \end{cases}$$

Step 4: The basic idea for factor scores is that a princi-

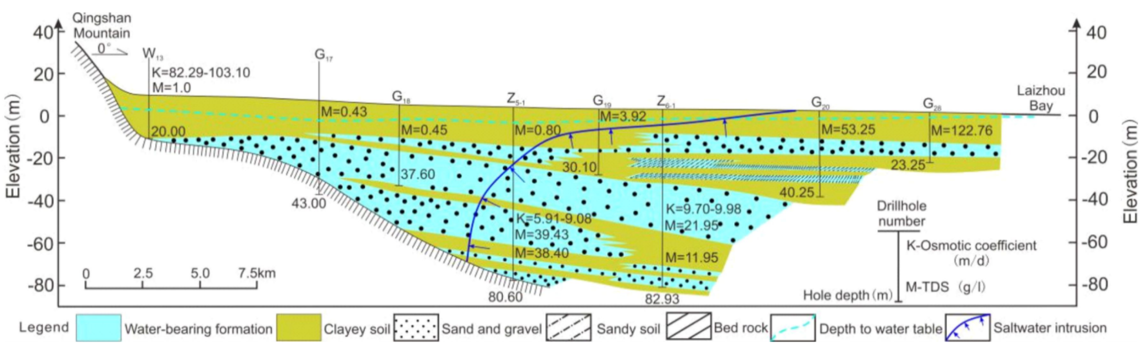

Fig. 1 Geologic section from Qingshan to Laizhou Bay in Mihe-Weihe River Basin.

pal factor is expressed as a linear combination of original variables, and factor scores are given by (Xue, 2015):

$$F_j = \beta_{j1}x_1 + \beta_{j2}x_2 + \ldots + \beta_{jp}x_p \, (j = 1, 2, \ldots, m)$$

3.2.2 Rough set theory

Definition 1: A decision information system S is expressed as $S = (U, C \cup D, V, f)$, where $U = (x_1, x_2, \ldots, x_n)$ is a non-empty finite set, i.e., domain. C and D are condition attribute set and decision attribute set respectively, and the intersection is empty. A binary equivalent relation $IND(B)$ is given by (Ma et al., 2022; Sawassi et al., 2022):

$$IND(B) = \{(x, y) \in U \times U \mid \forall a \in B, f(x, a) = f(y, a)\}$$

$U/IND(B)$ or U/B is an equivalence partition of U, and each equivalence partition is called a knowledge granularity.

Definition 2: $S = (U, C \cup D, V, f)$ is a decision information system, and for any attribute subset $B \subseteq C \cup D$, $U/IND(B) = \{X_1, X_2, \ldots, X_n\}$ represents a classification determined by a binary equivalent relation $IND(B)$. Information entropy $H(B)$ is defined as follows (Ma et al., 2022; Sawassi et al., 2022):

$$H(B) = -\sum_{i=1}^{n} p(X_i)\log_2 p(X_i)$$

where $p(X_i) = |X_i| / |U|$, $1 \leqslant i \leqslant n$, and $|X_i|$ is the base of X_i.

Definition 3: $S = (U, C \cup D, V, f)$ is a decision information system, and $U/IND(C) = \{X_1, X_2, \ldots, X_n\}$, $U/IND(D) = \{Y_1, Y_2, \ldots, Y_m\}$ are two classifications. Conditional entropy is defined as follows (Ma et al., 2022; Sawassi et al., 2022):

$$H(D|C) = -\sum_{i=1}^{n} p(X_i) \sum_{j=1}^{m} p(Y_j)\log_2 p(Y_j|X_i)$$

where $p(X_i) = |X_i| / |U|$, $p(Y_j|X_i) = \left|X_i \cap Y_j\right| / |X_i|$, $1 \leqslant i \leqslant n$, and $1 \leqslant j \leqslant m$.

Definition 4: $S = (U, C \cup D, V, f)$ is a decision information system, and $U/IND(C) = \{X_1, X_2, \cdots, X_n\}$, $U/IND(D) = \{Y_1, Y_2, \ldots, Y_m\}$ are two classifications. The mutual information between condition attribute C and decision attribute D is defined as follows (Ma et al., 2022; Sawassi et al., 2022):

$$I(C; D) = H(D) - H(D|C)$$

Definition 5: $S = (U, C \cup D, V, f)$ is a decision information system. For any attribute subset $B \subseteq C$, if $I(B; D) = I(C; D)$, $I(B - \{b\}; D) < I(C; D)$ $(b \in B)$, B is defined as a reduced set.

Definition 6: $S = (U, C \cup D, V, f)$ is a decision information system. For any attribute subset $B \subseteq C$, $a \in C - B$, the importance of attribute a is defined as follows (Ma et al., 2022; Sawassi et al., 2022):

$$sgn(a, B, D) = \frac{I(B \cup \{a\}; D) - I(B; D)}{H(D|\{a\})}$$

3.2.3 Improved matter element extension model

Compared with the traditional matter element extension model, there are two improvements: first, the classical domains and matter elements to be evaluated are normalized, and the matter-element distance is used instead of correlation functions, to solve the problem that correlation functions cannot be directly compared between different levels. Second, the close degree is used instead of maximum membership, to overcome defects of the maximum membership principle. Steps are as follows:

Step 1: Standardization of matter elements to be evaluated. The original matter elements divided by the maximum threshold $b_{pi} (i = 1, 2, \ldots, m)$ to obtain a new matter-element matrix R_0':

$$R_0' = (P_0, X_i, v_i') = \begin{bmatrix} P_0 & X_1 & v_1/b_{p1} \\ & X_2 & v_2/b_{p2} \\ \ldots & & \\ & X_m & v_m/b_{pm} \end{bmatrix}$$

Step 2: Standardization of classical domains. The original classical domains divided by the maximum threshold $b_{pi} (i = 1, 2, \ldots, m)$:

$$R_j' = \left(P_j, X_i, V_{ji}'\right) = \begin{bmatrix} P_j & X_1 & V_{j1}/b_{p1} \\ & X_2 & V_{j2}/b_{p2} \\ \ldots & & \\ & X_m & V_{jm}/b_{pm} \end{bmatrix} = \begin{bmatrix} P_j & X_1 & \langle s_{j1}, t_{j1} \rangle \\ & X_2 & \langle s_{j2}, t_{j2} \rangle \\ \ldots & & \\ & X_m & \langle s_{jm}, t_{jm} \rangle \end{bmatrix}$$

Step 3: The extension distance (D_{ji}) is given by (Cao and Bian, 2021):

$$D_{ji} = \left| V_i' - \frac{s_{ji} + t_{ji}}{2} \right| - \frac{t_{ji} - s_{ji}}{2}$$

Step 4: The closeness function is given by (Wang et al., 2020):

$$N = 1 - \frac{1}{m(m+1)} \sum_{i=1}^{m} w_i D$$

where N is the close degree, w_i is the weight, and D is the extension distance.

The above formula is applied to the improved matter element extension model, and the close degree is given by:

$$N_j'(P_0) = 1 - \frac{1}{m(m+1)} \sum_{i=1}^{m} w_i D_{ji}$$

Step 5: Based on the maximum closeness principle, the pollution degree caused by fluoride in groundwater is given by:

$$N_j'(P_0) = \max\left\{N_j'(P_0)\right\}$$

3.2.4 Fluoride contamination assessment

1) Contamination factor (*CF*)

The contamination factor (*CF*) is an index that is widely used to assess the pollution degree of single toxic element in groundwater or sediments (Hakanson, 1980; Antoniadis et al., 2019; Rinklebe et al., 2019). The *CF* is given by:

$$CF = \left(\frac{C_g}{C_{refg}}\right)$$

where C_g is the fluoride concentration in groundwater samples (mg/L). C_{refg} is the reference concentration in the Mihe-Weihe River Basin (mg/L). The *CF* is categorized as follows:

$$CF = \begin{cases} < 1, \text{ low contamination;} \\ 1-3, \text{ moderate contamination;} \\ 3-6, \text{ high contamination;} \\ \geqslant 6, \text{ very high contamination.} \end{cases}$$

2) Enrichment factor (*EF*)

The enrichment factor (*EF*) is used to assess the pollution degree in groundwater (Liaghati et al., 2004; Chen et al., 2015). The *EF* is given by:

$$EF = \frac{[C_i/C_{ib}]_{sample}}{[C_{re}/C_{reb}]_{RE}}$$

where *RE* is the concentration of the reference index. In this study, Zn is selected as the reference index. *sample* is the fluoride concentration. C_i is the fluoride concentration in groundwater samples (mg/L). C_{ib} is the reference concentration in the Mihe-Weihe River Basin (mg/L). C_{re} is the Zn concentration (mg/L). C_{reb} is the background concentration of Zn (mg/L). *EF* is categorized as follows:

$$EF = \begin{cases} \leqslant 1, \text{ RE concentration;} \\ 1-2, \text{ minimum enrichment;} \\ 2-5, \text{ moderate enrichment;} \\ 5-20, \text{ significant enrichment;} \\ 20-40, \text{ very high enrichment;} \\ > 40, \text{ extremely high enrichment.} \end{cases}$$

3) Geoaccumulation index (I_{geo})

Similar to the enrichment factor (*EF*), the geoaccumulation index (I_{geo}) is given by (Muller, 1969; Chakravarty and Patgiri, 2009; Chen et al., 2015):

$$I_{geo} = \log_2\left\{\frac{C_i}{1.5C_{bi}}\right\}$$

where C_i is the fluoride concentration in groundwater samples (mg/L), and C_{bi} is the background concentration in the Mihe-Weihe River Basin (mg/L). The I_{geo} is categorized as follows:

$$I_{geo} = \begin{cases} \leqslant 0, \text{ uncontaminated;} \\ 0-1, \text{ uncontaminated to moderately contaminated;} \\ 1-2, \text{ moderately contaminated;} \\ 2-3, \text{ moderately to heavily contaminated;} \\ 3-4, \text{ heavily contaminated;} \\ 4-5, \text{ heavily to extremely contaminated;} \\ > 5, \text{ extremely contaminated.} \end{cases}$$

3.2.5 Fluoride ecological risk assessment

The ecological risks were evaluated by the monomial potential ecological risk index (*E*) (Yi et al., 2011; Gholizadeh and Patimar, 2018; Dang et al., 2021). The *E* is given by:

$$E = T \times CF = T \times \left(\frac{C_g}{C_{refg}}\right)$$

where *T* is the toxic response factor, and *T* is determined by toxicology as 5 (Lin, 2009). C_g is the fluoride concentration in groundwater samples (mg/L). C_{refg} is the background concentration in the Mihe-Weihe River Basin (mg/L). The *E* is classified as:

$$E = \begin{cases} < 40, \text{ low potential ecological risk;} \\ 40-80, \text{ moderate potential ecological risk;} \\ 80-160, \text{ considerable potential ecological risk;} \\ 160-320, \text{ high potential ecological risk;} \\ \geqslant 320, \text{ very high potential ecological risk.} \end{cases}$$

3.2.6 Fluoride health risk assessment

Ingestion and dermal contact are the major ways for adults and children to be exposed to fluoride in groundwater (De Miguel et al., 2007; Wu et al., 2009). Non-carcinogenic risk indexes (*HQ* and *HI*) are adopted to evaluate the health risks caused by fluorine pollution in groundwater. *HQ* and *HI* are given by:

$$HI = \underbrace{\left(\frac{ADD_{\text{ingestion}}}{RfD_{\text{ingestion}}}\right)}_{(HQ-\text{ingestion})} + \underbrace{\left(\frac{ADD_{\text{dermal}}}{RfD_{\text{dermal}}}\right)}_{(HQ-\text{dermal})}$$

$$ADD_{\text{ingestion}} = \frac{C_w \times IR \times EF \times ED}{BW \times AT}$$

$$ADD_{\text{dermal}} = \frac{C_w \times SA \times K_p \times ET \times EF \times ED \times 10^{-3}}{BW \times AT}$$

In this study, $RfD_{\text{ingestion}}$=40 μg/(kg·d) and RfD_{dermal}=40μg/(kg·d) (USEPA, 1989; USEPA, 2002b). For adults, *IR*=2 L/d, *EF*=350 d/a, *ED*=30 a, *BW*=70 kg, *AT*=*ED*×365 d, *SA*=18000 cm^2, K_p=0.001 cm/h, *ET*=0.58 h/d. For children, *IR*=0.64 L/d, *EF*=350 d/a, *ED*=6 a, *BW*=15 kg, *AT*=*ED*×365 d, *SA*=6600 cm^2, K_p=0.001 cm/h, *ET*=1 h/d (Muller, 1969; Hakanson. 1980; USEPA, 1989, 1993, 1997, 2002a; WHO, 1993). The *HQ* or *HI* is classified as (USEPA, 1989):

$$HQ/HI = \begin{cases} < 1, \text{fewer or no non-carcinogenic health problems;} \\ > 1, \text{more non-carcinogenic health problems.} \end{cases}$$

4 Results and discussion

4.1 Hydrochemical characteristics

Statistics (Min, Max, Mean, Std., and CV%) for the wet season (n = 87) and dry season (n = 92) are shown in Table 1. In the wet season, pH ranged from 7.08 to 8.28, and TDS varied from 345 to 2285 mg/L. HCO_3^-, the main anion, varied from 164.5 to 677.5 mg/L, and Ca^{2+}, Mg^{2+}, the main cations, varied from 7.76 to 386.4 mg/L and 6.35 to 164.7 mg/L. Samples 7, 12, 14, 16, 17, 18, 20, 26, and 99 are located in the northeastern part of the study area and are the sodium type.

In the dry season, pH ranged from 6.80 to 11.11, and TDS varied from 355.88 to 5688.72 mg/L (Table 1). Similarly, HCO_3^-, the main anion, varied from 125.1 to 825.99 mg/L, and Ca^{2+}, Mg^{2+} were the main cations, from 6.88 to 395.33 mg/L and 0.12 to 180.89 mg/L.

4.2 Spatial distribution of fluoride

4.2.1 Transversal distribution characteristics

Fluoride concentration in groundwater during the wet season ranged from 0.22 to 8.49 mg/L (n = 87, Table 2), of which 16.09% of the samples were greater than 1.00 mg/L, mainly located in the Changyi and Weihe water source areas. The maximum [F^-] of 8.49 mg/L was found in Changyi water source area. These high-fluoride samples (n = 14) are mainly HCO_3·Cl-Na (42.86%) and HCO_3-Na (21.43%) (Fig. 2(a)), and the low-fluoride samples (n = 35) are mainly HCO_3·SO_4·Cl-Ca (28.57%), near the Weihe River.

Fluoride concentration in groundwater during the dry season ranged from 0.19 to 6.48 mg/L (n = 92, Table 2), of which 8.70% of the samples were greater than 1.00 mg/L, also located in the Changyi and Weihe water source areas. The maximum [F^-] of 6.48 mg/L was also found in sy026. These high-fluoride samples (n = 8) are HCO_3·Cl-Na and HCO_3-Na (Fig. 2(b)), and the low-fluoride samples (n = 65) are HCO_3·SO_4·Cl-Ca and HCO_3·Cl-Ca·Mg (Fig. 2(b)), near the Mihe River and Weihe River.

Table 1 Statistics of hydrochemical indexes for groundwater samples from wet season and dry season (n_1=87 and n_2=92)

Season	Statistics	Parameters										
		pH	TDS (mg/L)	K^+ (mg/L)	Na^+ (mg/L)	Ca^{2+} (mg/L)	Mg^{2+} (mg/L)	Cl^- (mg/L)	SO_4^{2-} (mg/L)	HCO_3^- (mg/L)	NO_3^- (mg/L)	F^- (mg/L)
Wet season	Min	7.08	345.00	0.42	14.41	7.76	6.35	18.55	8.39	164.50	0.22	3.70
	Max	8.28	2285.00	20.04	731.30	386.40	164.70	900.60	646.70	677.50	8.49	816.60
	Mean	7.52	1083.60	3.47	130.04	167.48	47.00	183.79	151.75	364.50	0.79	214.70
	Std.	0.27	401.23	4.38	119.07	82.94	26.56	123.90	95.88	108.40	1.00	169.23
Dry season	Min	6.80	355.88	0.49	13.07	6.88	0.12	23.09	8.73	125.10	0.19	5.37
	Max	11.11	5688.72	84.01	1579.41	395.33	180.89	2529.23	699.81	825.99	6.48	739.17
	Mean	7.50	1089.85	4.83	129.13	169.85	48.07	190.75	139.55	373.50	0.57	200.49
	Std.	0.51	637.69	10.43	193.29	86.24	30.96	277.03	102.36	125.70	0.78	171.34

Notes: wet season CV (%): pH 3.65; TDS 37.03; K^+ 79.33; Na^+ 91.57; Ca^{2+} 49.52; Mg^{2+} 56.51%; Cl^- 67.42; SO_4^{2-} 63.18; HCO_3^- 29.75; NO_3^- 79.28; F^- 78.82. dry season CV (%): pH 6.77; TDS 58.51; K^+ 46.28; Na^+ 66.80; Ca^{2+} 50.78; Mg^{2+} 64.40%; Cl^- 68.86; SO_4^{2-} 73.35; HCO_3^- 33.65; NO_3^- 72.86; F^- 85.46.

Table 2 Statistics of fluoride concentration in wet season and dry season

Season	Statistics	Classifications of fluorine content in groundwater (mg/L)			Total
		Low fluorine water(F^-<0.50)	Medium fluorine water(0.50≤F^-≤1.00)	High fluorine water(F^->1.00)	
Wet season	Numbers	35.00	38.00	14.00	87.00
	Min/Max	0.22/0.49	0.50/0.94	1.09/8.49	0.22/8.49
	Mean	0.38	0.62	2.29	0.79
	Std.	0.07	0.11	1.90	1.00
Dry season	Numbers	65.00	19.00	8.00	92.00
	Min/Max	0.19/0.49	0.50/0.92	1.09/6.48	0.19/6.48
	Mean	0.32	0.67	2.35	0.57
	Std.	0.07	0.14	1.87	0.78

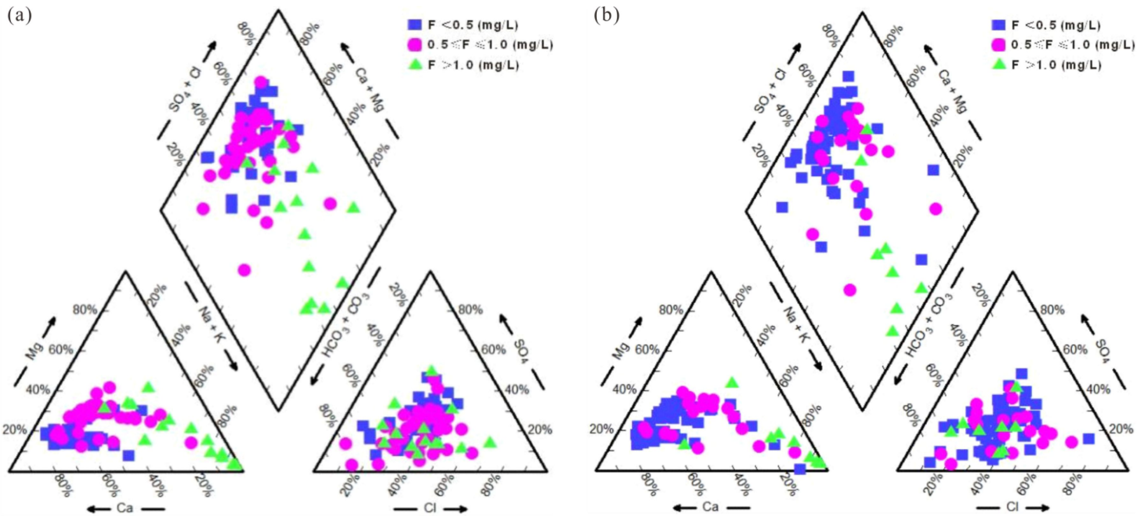

Fig. 2 (a) Piper diagram expressing hydrochemical characteristics in wet season. (b) Piper diagram expressing hydrochemical characteristics in dry season.

4.2.2 Vertical distribution characteristics

In the wet season, the depth to the water table of high-fluorine water ($F^- > 1.00$ mg/L) is in the range of 30–45 m, the maximum up to 8.49 mg/L, and fluoride concentration changes greatly in the vertical direction (Figs. 3(a) and 3(b)). In the dry season, the depth to the water table of high-fluorine water is in the range of 25–40 m, with a maximum of 6.48 mg/L, and fluoride concentration shows less changes in vertical direction (Figs. 3(c) and 3(d)). However, as the depth to the water table varies from 0 to 60 m, the fluorine content increases slightly in both wet season and dry season (wet season > dry season (Fig. 4(a))). This variation may be caused by selection bias, because most samples were collected from shallow aquifers at depths less than 60 m (Fig. 4(b)).

4.3 Factors influencing fluorine enrichment in groundwater

4.3.1 Relationship between the fluoride concentration and microlandforms

A total of 179 samples (in the wet and dry seasons) were selected. The fluoride concentration in shallow groundwater is closely related to topographic features, and there is a negative correlation between the fluoride concentration in groundwater and ground height; that is, as the ground height decreases, the fluorine content in groundwater increases gradually (Fig. 4(c)). The microlandform is divided into interfluvial lowlands, alluvial-marine plains and piedmont alluvial fans, and fluoride concentration ranged from 0.88 to 0.42 mg/L in wet season, 0.65 to 0.22 mg/L in dry season. It can be concluded that hydrodynamic conditions are improving from flat to steep, water-rock interaction in short times, and the dissolved fluorine content in the groundwater decreases, not conducive to fluorine enrichment.

4.3.2 Relationship between the fluoride concentration and pH

As shown in Fig. 4(d), high-fluorine groundwater ($F^- >$ 1.00 mg/L) in the Mihe-Weihe River Basin is weakly alkaline. pH in high-fluorine samples taken during the wet season varied from 7.47 to 8.28 and from 7.10 to 8.02 in the dry season. As alkaline enhanced, fluoride concentration also increased gradually, showing a significant positive correlation. The reason for this increase is that in the weakly alkaline environment, the chemical properties of fluoride are very active, but the charges on the surfaces of sedimentary minerals are neutral or negative, decreasing the adsorption of fluoride, while prone to displacement reaction between OH^- and F^-. This process can release F^- into the groundwater, conducive to fluorine enrichment (Du et al., 2011).

4.3.3 Relationship between the fluoride concentration and TDS

TDS varied from 345 to 2285 mg/L in the wet season, with an average of 1078.30 mg/L and a coefficient of variation of 37.21%. TDS varied from 356 to 5689 mg/L in the dry season, with an average of 1089.85 mg/L and a coefficient of variation of 58.51%. There is no obvious correlation between TDS and high-fluoride groundwater. Samples in the southwestern part are fresh water with TDS less than 1.00 g/L, but fluorine concentration up to 1.55 mg/L in wet season and 3.66 mg/L in dry season. In other regions, TDS varied greatly, but fluoride concentration mainly ranged from 0.00 to 1.00 mg/L (Fig. 5). It can be concluded that high-fluorine groundwater in the Mihe-

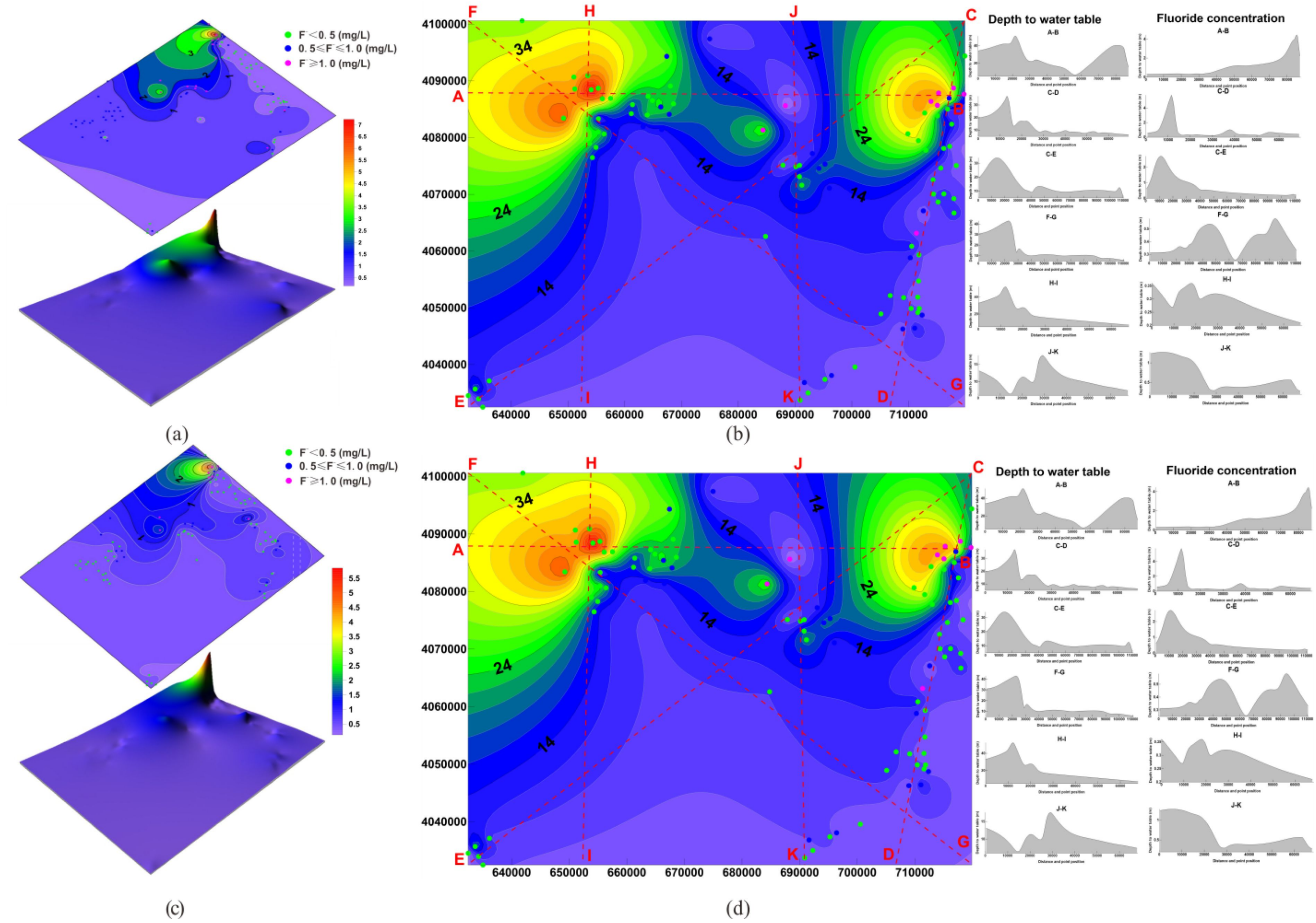

Fig. 3 (a) Spatial distribution characteristics of fluoride in wet season. (b) Vertical distribution characteristics of fluorine content in wet season. (c) Spatial distribution characteristics of fluoride in dry season. (d) Vertical distribution characteristics of fluorine content in dry season.

Weihe River Basin is mainly controlled by the fluorine-containing minerals.

4.3.4 Relationship between the fluoride concentration and other major ions

Figs. 6(a) and 6(b) show that fluoride concentration is negatively correlated with Ca^{2+} and Mg^{2+}, indicating that fluoride is easily enriched with low concentrations of Ca^{2+} and Mg^{2+}. In contrast, fluorine richness is inhibited with high Ca^{2+} and Mg^{2+} concentration. Cl^- and SO_4^{2-} are sensitive ions that change with the environment and are mainly affected by human activities. There is no obvious correlation between the fluoride content in groundwater and Cl^-, SO_4^{2-} in the study area (Figs. 6(c) and 6(d)). It shows that human activities are not the major cause of excessive fluoride in groundwater. There is a positive correlation between $\rho(F^-)$ and $\rho(Na^+)/(\rho(Na^+)+\rho(Ca^{2+}))$, $\rho(F^-)$ and $c(HCO_3^-)-c(Ca^{2+})-c(Mg^{2+})$ (Figs. 6(e) and 6(f)), suggesting that weakly alkaline with high HCO_3^- and Na^+ concentration is favorable for fluorine richness.

4.4 Mechanism of fluorine richness in groundwater

4.4.1 Rock weathering and evaporation

As shown in Figs. 7(a) and 7(b), a small portion of groundwater samples ($F^- < 0.50$ mg/L and $0.50 \leqslant F^- \leqslant 1.00$ mg/L) are controlled by rock weathering, while samples change from rock weathering dominance to evaporation-crystallization dominance as fluoride concentration greater than 1.00 mg/L, indicating that evaporation-crystallization may be a reason for fluorine richness.

4.4.2 Hydrogeochemical modeling of dissolution and precipitation for fluorine-containing minerals (fluorite)

Log[Ca^{2+}]activity, Log[F^-]activity, $SI_{Calcite}$ and $SI_{Fluorite}$ were calculated by PHREEQC. As shown in Fig. 7(c), $SI_{Fluorite}$ is less than 0, in an unsaturated condition, and there is an exponential relationship between $SI_{Fluorite}$ and fluoride concentration, meaning that the fluoride in groundwater of Mihe-Weihe River Basin is mainly from

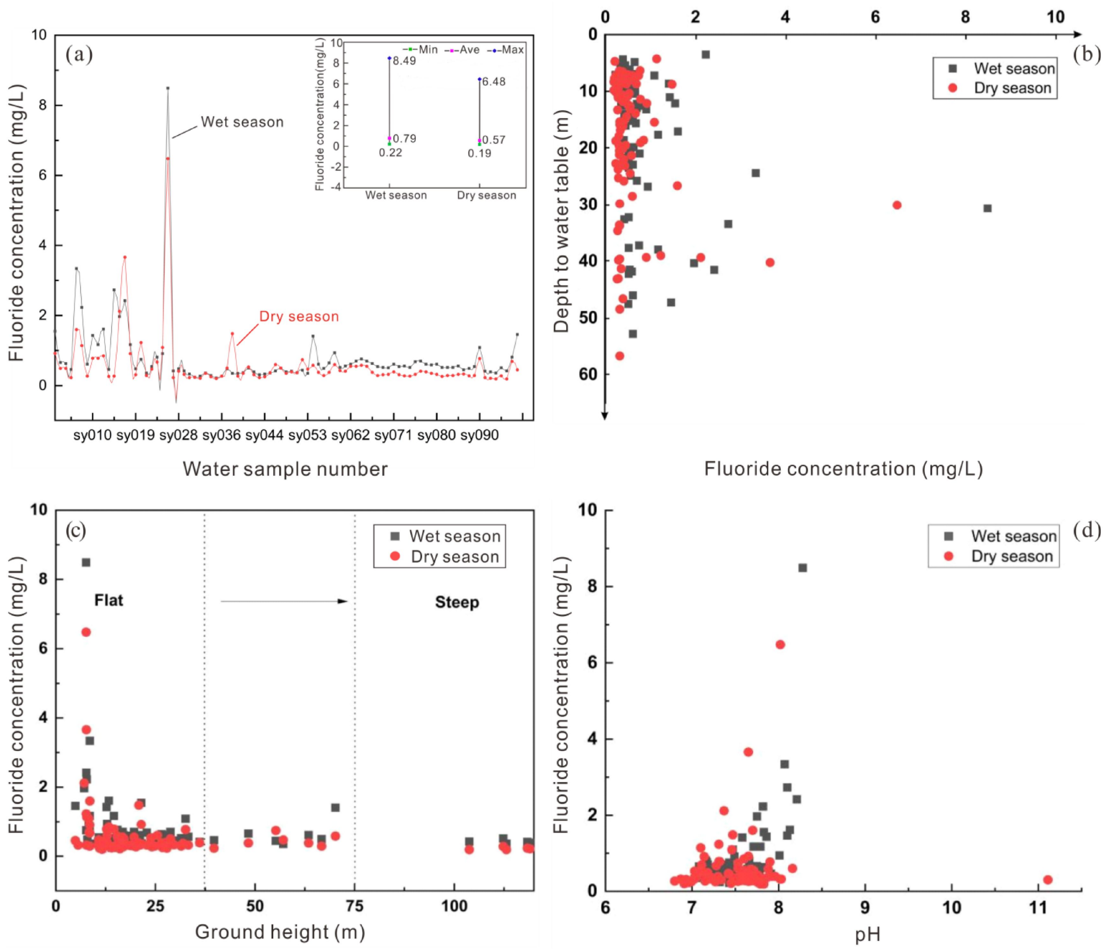

Fig. 4 (a) Comparison of fluorine content in groundwater during wet season and dry season. (b) Relationship between fluoride concentration and depth to water table. (c) Relationship between fluorine content in groundwater and ground height. (d) Relationship between fluoride concentration and pH.

the dissolution of fluorite and other fluorine-containing minerals. As shown in Fig. 7(d), $SI_{Calcite}$ is basically greater than 0, in a supersaturation condition, meaning that fluoride concentration is restricted by the Calcium concentration, and there is a negative correlation between Ca^{2+} (%) and fluoride concentration (Fig. 7(e)). Fig. 7(f) shows that all samples are below the stability line ($\lg k$ = 10.6), suggesting that fluorine richness in the Mihe-Weihe River Basin is jointly controlled by the dissolution of fluorine-containing minerals (fluorite) and calcium-containing minerals (calcite). If only fluorite is dissolved, log[F^-] activity and log[Ca^{2+}] activity all increase along trend line 1. If both calcite and fluorite are dissolved and the calcite-to-fluorite quality ratio is 200:1, log[F^-] activity and log[Ca^{2+}] activity increase along trend line 2. If there are cation exchange and calcite precipitation, log[F^-] activity and log[Ca^{2+}] activity will evolve along trend line 3 (Fig. 7(f)).

Some samples are located between trend lines 1 and 2 and are closer to trend line 2, which indicates that fluoride concentration is controlled by Ca^{2+} originating from the dissolution of fluorite and calcite, a state of fluorite and calcite dissolving together with a fluorite-to-calcite quality ratio greater than 1:200. Some samples, with a fluorite-to-calcite quality ratio less than 1:200, are located at the bottom right of trend line 2 (Fig. 7(f)), which indicates that through eluviation, fluoride in fluorine-containing minerals enters groundwater and continuously accumulates with other components through evaporation and concentration, resulting in excessive fluoride in groundwater of Mihe-Weihe River Basin.

4.5 Main factors controlling fluorine richness in groundwater

The main factors influencing fluorine richness were analyzed by factor analysis, and the main controlling factors were revealed. Seven indexes (Na^+, Ca^{2+}, Mg^{2+}, HCO_3^-, pH, F^-, and ground height) were selected, and the results of KMO and Bartlett's test are shown in Table 3. For the wet season data, the results of the KMO and Bartlett's test are 0.720 and 208.249 (P < 0.001), and for

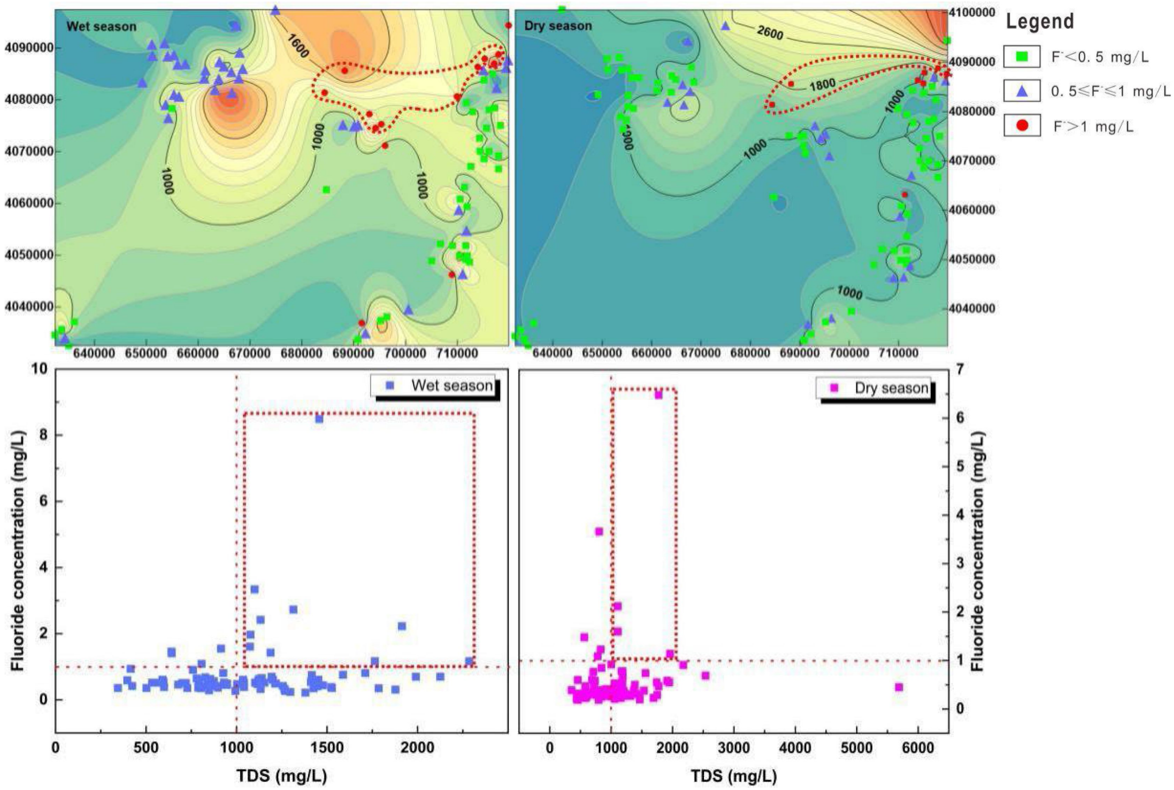

Fig. 5 Relationship between fluoride concentration and TDS.

dry season, they are 0.568 and 162.525 ($P < 0.001$). So the original data are suitable for PCA dimensional reduction.

Based on cumulative variances of rotated common factors greater than 50%, the first and second factors controlling fluorine richness in the wet season are identified as Ca^{2+}, pH and HCO_3^-, Mg^{2+}, Na^+, ground height. Similarly, the first factor controlling fluorine richness in the dry season includes HCO_3^-, Na^+, ground height and the second factor includes Ca^{2+}, Mg^{2+}, pH (Table 3). PCA modeling is shown as follows:

Wet season:

$$F_1 = 0.345\mathrm{pH} + 0.124\mathrm{Na}^+ - 0.378\mathrm{Ca}^{2+} - 0.329\mathrm{Mg}^{2+} - 0.071\mathrm{HCO}_3^- + 0.228\mathrm{F}^- - 0.054\mathrm{H}$$

$$F_2 = -0.041\mathrm{pH} + 0.292\mathrm{Na}^+ + 0.121\mathrm{Ca}^{2+} + 0.458\mathrm{Mg}^{2+} + 0.424\mathrm{HCO}_3^- + 0.153\mathrm{F}^- - 0.198\mathrm{H}$$

Dry season:

$$F_1 = -0.066\mathrm{pH} + 0.333\mathrm{Na}^+ - 0.115\mathrm{Ca}^{2+} + 0.166\mathrm{Mg}^{2+} + 0.361\mathrm{HCO}_3^- + 0.296\mathrm{F}^- - 0.236\mathrm{H}$$

$$F_2 = -0.351\mathrm{pH} + 0.051\mathrm{Na}^+ + 0.449\mathrm{Ca}^{2+} + 0.380\mathrm{Mg}^{2+} + 0.015\mathrm{HCO}_3^- - 0.274\mathrm{F}^- - 0.091\mathrm{H}$$

For the wet season, the contribution rate of the first principal factor is 35.732%, and the first principal factor is strongly negatively correlated with Ca^{2+}, strong positive correlations with pH and F^-, which indicates that in a weakly alkaline environment, the dissolution of Ca^{2+} is inhibited due to fluorine richness in groundwater during the wet season. The activity of Ca^{2+} decreases, which is beneficial to fluorine richness in groundwater, and the high fluoride content in groundwater is mainly from the dissolution of fluorine-containing minerals. The contribution rate of the second principal factor is 28.739%, and there are strong positive correlations between the second principal factor and HCO_3^-, Mg^{2+}, Na^+. A medium-negative correlation exists between the second principal factor and ground height. Therefore, in low-lying areas, fluorine richness in groundwater is controlled by rock weathering, evaporation and concentration. Dolomite dissolution becomes the major source of ion components in groundwater, and by evaporation and concentration, F^- is concentrated with other ion components.

In the dry season, the contribution rate of the first principal factor is 33.220%, and there are strong positive correlations between the first principal factor and HCO_3^-, Na^+, F^-. A medium-negative correlation exists between the first principal factor and ground height. This shows that in the dry season, F^- is mainly enriched in low-lying areas with weak alkaline environments that are rich in sodium and poor in calcium. The contribution rate of the second principal factor is 25.743%, and there are strong

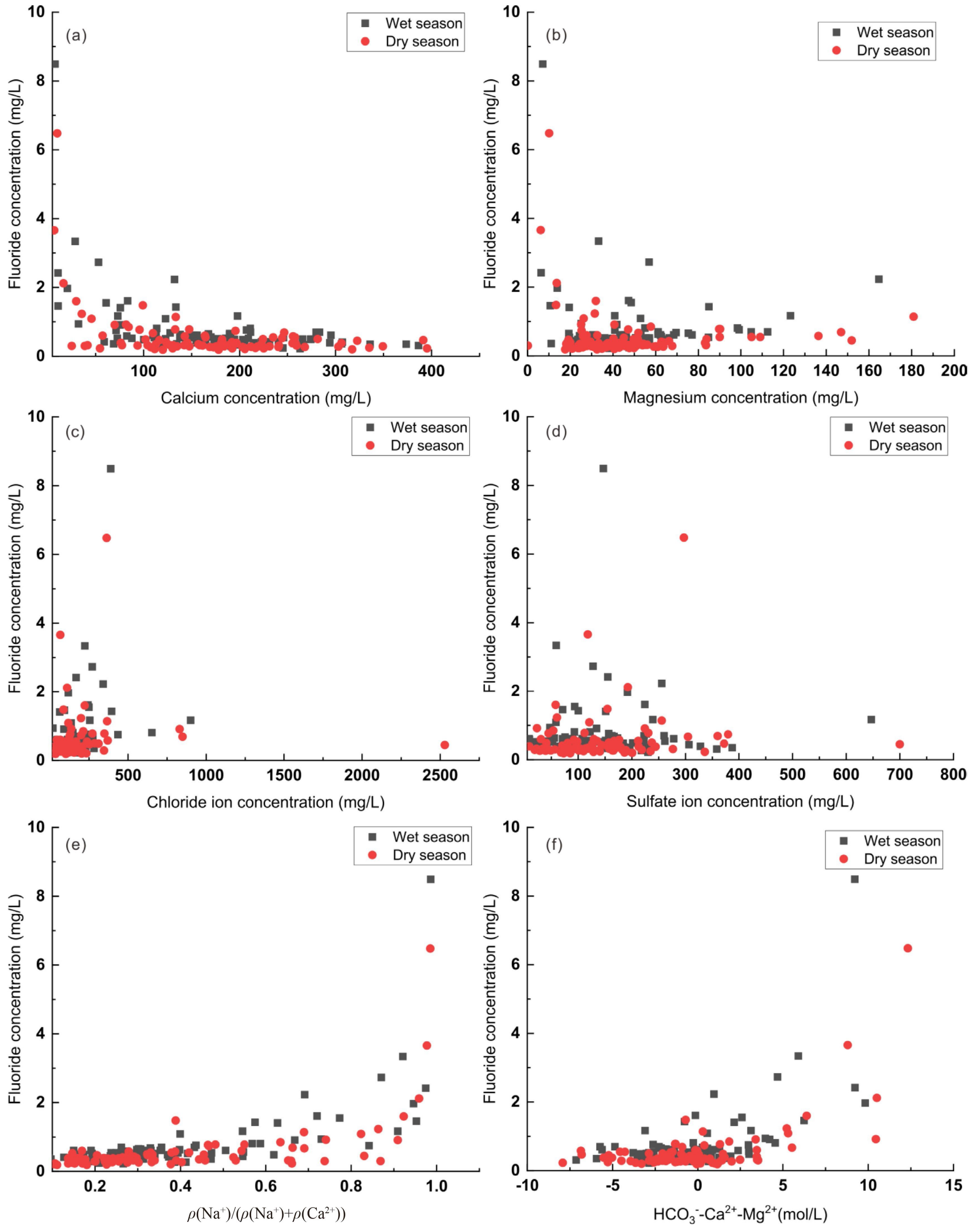

Fig. 6 (a) Relationship between fluoride concentration and Ca^{2+}. (b) Relationship between fluoride concentration and Mg^{2+}. (c) Relationship between fluoride concentration and Cl^{-}. (d) Relationship between fluoride concentration and SO_4^{2-}. (e) Relationship between fluoride concentration and Na^{+}. (f) Relationship between fluoride concentration and HCO_3^{-}.

positive correlations between the second principal factor and Ca^{2+}, Mg^{2+}. A medium-negative correlation exists between the second principal factor and F^{-}, and a strong negative correlation exists between the second principal factor and pH. It is shown that fluorine richness in groundwater is inhibited by rock weathering and the dissolution of Ca^{2+} during the dry season, while in a weakly alkaline environment, the activity of Ca^{2+} decreases, which is beneficial to fluorine richness in groundwater, but the former plays a dominant role.

In summary, fluorine richness in groundwater during the wet season in Mihe-Weihe River Basin is mainly controlled by the dissolution of fluorine-containing minerals, followed by the effects of evaporation and

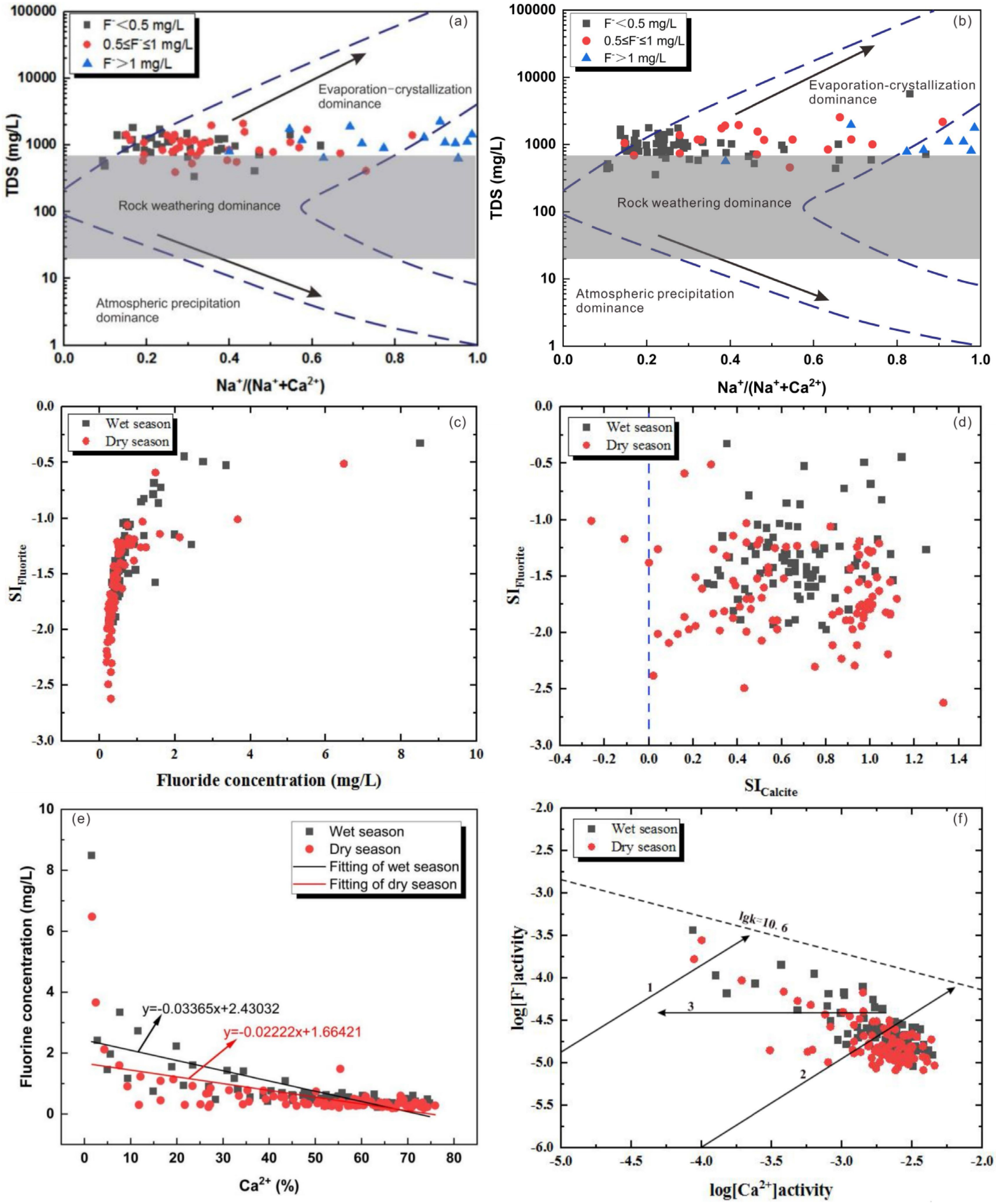

Fig. 7 (a) Relationship between $Na^+/(Na^++Ca^{2+})$ and TDS in wet season. (b) Relationship between $Na^+/(Na^++Ca^{2+})$ and TDS in dry season. (c) Relationship between fluoride concentration and $SI_{Fluorite}$. (d) Relationship between $SI_{Calcite}$ and $SI_{Fluorite}$. (e) Relationship between Ca^{2+} (%) and fluoride concentration. (f) Relationship between log[Ca^{2+}] activity and log[F^-] activity.

concentration. In the dry season, F^- is mainly concentrated in the low-lying areas with weak alkaline environments that are rich in sodium and poor in calcium, but at the same time, it is also inhibited by rock weathering and the dissolution of Ca^{2+}. Combined with the influence of hydrodynamic factors, the above results result in the differences in fluoride concentration at the same sampling point during the wet season and dry season in the Mihe-Weihe River Basin (Figs. 8(a), 8(b) and 4 (a)).

4.6 Contamination and risk assessment

4.6.1 Contamination factor (*CF*), Enrichment factor (*EF*) and geoaccumulation index (I_{geo})

As shown in Figs. 9(a) and 10(a), the *CF* values mainly between 0 and 1 (low contamination), moderate contamination (1 < *CF* < 3) occurs locally, and few samples are heavily contaminated. In addition, the pollution range in wet season can be observed more

Table 3 Principal components for fluorine richness in groundwater during wet season and dry season in Mihe-Weihe River Basin.

Indices	Wet season Principal components		Dry season Principal components	
	1	2	1	2
Ca^{2+} (mg/L)	−0.859	−0.028	−0.263	0.808
pH	0.834	0.165	−0.158	−0.633
F^- (mg/L)	0.679	0.471	0.685	−0.490
HCO_3^- (mg/L)	0.128	0.803	0.840	0.031
Mg^{2+} (mg/L)	−0.493	0.686	0.391	0.686
Na^+ (mg/L)	0.520	0.676	0.776	0.095
Ground height (m)	−0.276	−0.438	−0.549	−0.166
Eigenvalue	3.015	1.498	2.326	1.802
Variance contribution (%)	35.732	28.739	33.220	25.743
Accumulating contribution rate (%)	35.732	64.471	33.220	58.963

Notes: Wet season: Kaiser-Meyer-Olkin: 0.720, Bartlett: 208.249, df: 21, Sig.: 0; Dry season: Kaiser-Meyer-Olkin: 0.568, Bartlett: 162.525, df: 21, Sig.: 0.

widely than dry season; as a result, the wet season is recorded as the season with the maximum effects on groundwater, while the dry season remains less affected. As shown in Figs. 9(b) and 10(b), most *EF* values are higher (more than 5), except for some samples in the east. Besides, wet season or dry season, *EF* reveals the maximum enrichment near the Laizhou Bay, suggesting that hydrodynamic factors have a significant impact on the enrichment of F^- in groundwater. As shown in Figs. 9 (c) and 10(c), the I_{geo} values are less than 0 (uncontaminated) for most samples, greater than 0 (contaminated) only in Weihan and Changyi water source areas, and compared with the dry season, the groundwater is more seriously polluted in wet season.

4.6.2 Comprehensive model for evaluating fluoride pollution in groundwater

Uncertain knowledge representation and processing are involved in the evaluation of fluoride pollution in groundwater. Rough set theory and the improved matter element extension model are used to define the pollution degree. The processes are as follows:

Step 1: Determination of matter elements to be evaluated.

The standardized matter element matrices are constructed as follows:

Wet season:

$$R'_{p1}=\begin{bmatrix} Np & CF & 0.18\\ & EF & 1.00\\ & I_{geo} & 0.02\end{bmatrix},\ R'_{p2}=\begin{bmatrix} Np & CF & 0.08\\ & EF & 0.34\\ & I_{geo} & -0.47\end{bmatrix},\ R'_{p3}=\begin{bmatrix} Np & CF & 0.07\\ & EF & 0.01\\ & I_{geo} & -0.50\end{bmatrix}\cdots R'_{p87}=\begin{bmatrix} Np & CF & 0.17\\ & EF & 0.75\\ & I_{geo} & -0.02\end{bmatrix}$$

Dry season:

$$R'_{p1}=\begin{bmatrix} Np & CF & 0.05\\ & EF & 0.01\\ & I_{geo} & -1.10\end{bmatrix},\ R'_{p2}=\begin{bmatrix} Np & CF & 0.05\\ & EF & 0.04\\ & I_{geo} & -1.10\end{bmatrix},\ R'_{p3}=\begin{bmatrix} Np & CF & 0.14\\ & EF & 0.17\\ & I_{geo} & -0.33\end{bmatrix}\cdots R'_{p92}=\begin{bmatrix} Np & CF & 0.07\\ & EF & 0.09\\ & I_{geo} & -0.83\end{bmatrix}$$

Step 2: Determination of the classical domain and node domain.

Indexes are divided into six levels, namely, no, low, moderate, high, very high and extremely high concentrations. The standardized classical domain and node domain are determined as follows:

Standardized classical domain:

$$R'_j=\begin{bmatrix} P & P_1 & P_2 & P_3 & P_4 & P_5 & P_6\\ CF & \langle 0,0.118\rangle & \langle 0.118,0.353\rangle & \langle 0.353,0.707\rangle & \langle 0.707,1\rangle & & \\ EF & \langle 0,0.00103\rangle & \langle 0.00103,0.00206\rangle & \langle 0.00206,0.00516\rangle & \langle 0.00516,0.0206\rangle & \langle 0.0206,0.0413\rangle & \langle 0.0413,1\rangle\\ I_{geo} & \langle -1.108,0\rangle & \langle 0,0.4\rangle & \langle 0.4,0.8\rangle & \langle 0.8,1\rangle & & \end{bmatrix}(wet\ season)$$

$$R'_j=\begin{bmatrix} P & P_1 & P_2 & P_3 & P_4 & P_5 & P_6\\ CF & \langle 0,0.154\rangle & \langle 0.154,0.463\rangle & \langle 0.463,0.926\rangle & \langle 0.926,1\rangle & & \\ EF & \langle 0,0.000559\rangle & \langle 0.000559,0.00112\rangle & \langle 0.00112,0.00279\rangle & \langle 0.00279,0.0112\rangle & \langle 0.0112,0.0223\rangle & \langle 0.0223,1\rangle\\ I_{geo} & \langle -1.412,0\rangle & \langle 0,0.474\rangle & \langle 0.474,0.948\rangle & \langle 0.948,1\rangle & & \end{bmatrix}(dry\ season)$$

Standardized node domain:

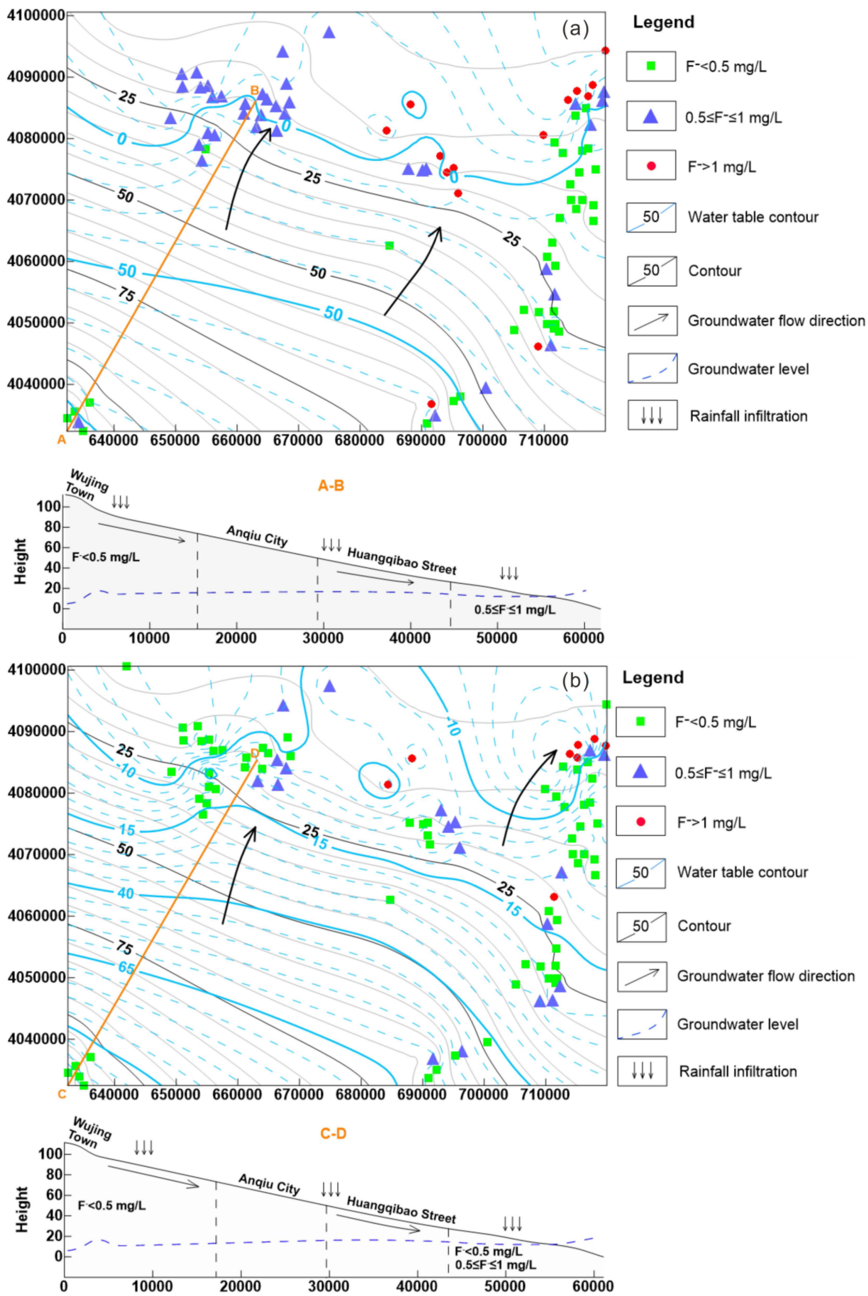

Fig. 8 (a) Pattern graph of fluorine richness in wet season. (b) Pattern graph of fluorine richness in dry season.

$$R_p = \begin{bmatrix} NpCF\langle 0,1\rangle \\ EF\langle 0,1\rangle \\ I_{geo}\langle -1.108,1\rangle \end{bmatrix} (wet\ season),\ R_p = \begin{bmatrix} NpCF\langle 0,1\rangle \\ EF\langle 0,1\rangle \\ I_{geo}\langle -1.412,1\rangle \end{bmatrix} (dry\ season)$$

Step 3: Calculation of the extension distance.

The extension distance (D_{ji}) is calculated by

$$R'_j = \left(P_j, X_i, V'_{ji}\right) = \begin{bmatrix} P_j X_1 V_{j1}/b_{p1} \\ X_2 V_{j2}/b_{p2} \\ \cdots \\ X_m V_{jm}/b_{pm} \end{bmatrix} = \begin{bmatrix} P_j X_1\langle s_{j1}, t_{j1}\rangle \\ X_2\langle s_{j2}, t_{j2}\rangle \\ \cdots \\ X_m\langle s_{jm}, t_{jm}\rangle \end{bmatrix} \text{ and } D_{ji} = \left|V'_i - \frac{s_{ji}+t_{ji}}{2}\right| - \frac{t_{ji}-s_{ji}}{2}.$$

Taking SY01 as an example, the results are shown in Table 4.

Step 4: Calculation of the index weights.

The index weights were determined by rough set theory, and the equivalence partition of domain U is given by:

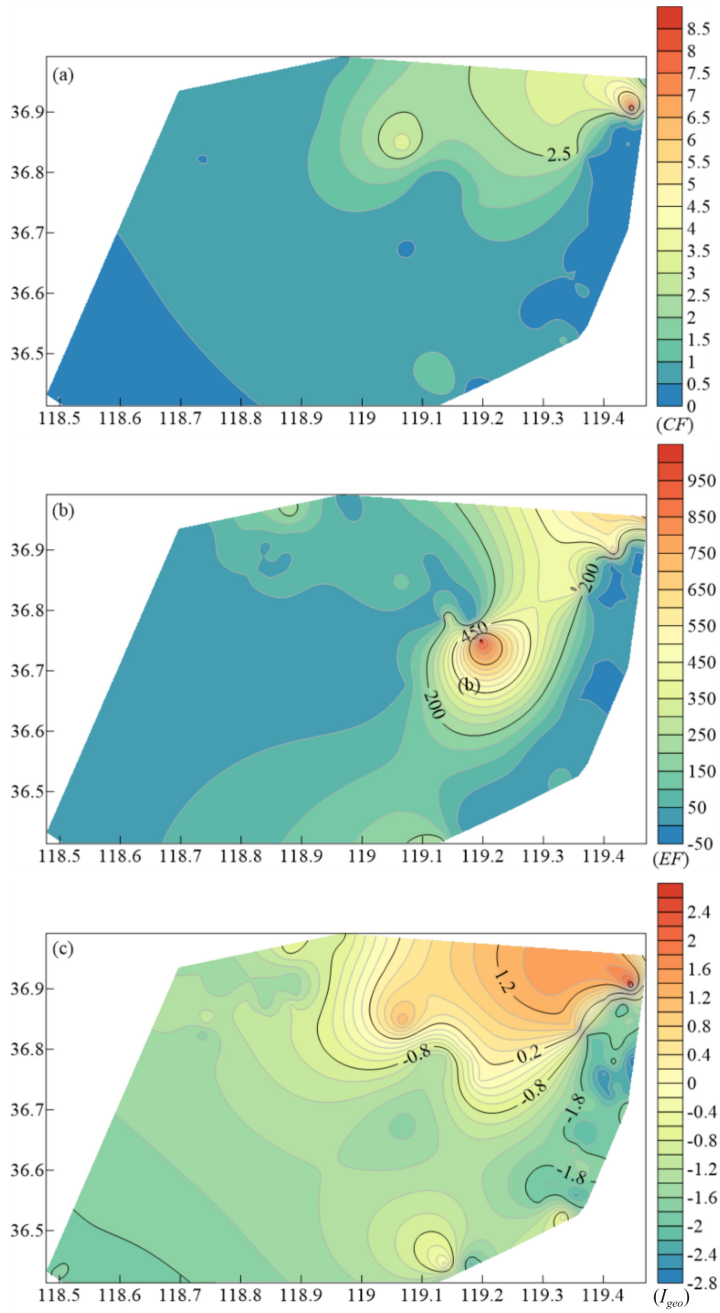

Fig. 9 Contamination assessment in wet season. (a) *CF*; (b) *EF*; (c) I_{geo}.

Wet season:

$$\frac{U}{ind(X)} = \left\{\begin{array}{l} \{SY1, SY10, SY12, SY13, SY14\}, \{SY2, SY50, SY51, SY53, SY54, SY55, SY57, SY58, SY59, SY62, SY64, SY66, SY68\} \\ \left\{\begin{array}{l} SY3, SY11, SY17, SY19, SY25, SY26, SY28, SY29, SY36, SY37, SY42, SY45, SY47, SY48, SY52, SY60, SY65, SY69 \\ SY72, SY78, SY82, SY83, SY84 \end{array}\right\} \\ \{SY4, SY7, SY18, SY56, SY61, SY63, SY67, SY70, SY71, SY73, SY74, SY75, SY76, SY77, SY79, SY85, SY86\} \\ \{SY5\}, \{SY6\}, \{SY8, SY9\}, \{SY15, SY49, SY80, SY87\}, \{SY16, SY23\}, \{SY20, SY31, SY35, SY39, SY46, SY81\} \\ \{SY21, SY24, SY27, SY30, SY32, SY33, SY34, SY38, SY40, SY41, SY43, SY44\}, \{SY22\} \end{array}\right\}$$

Dry season:

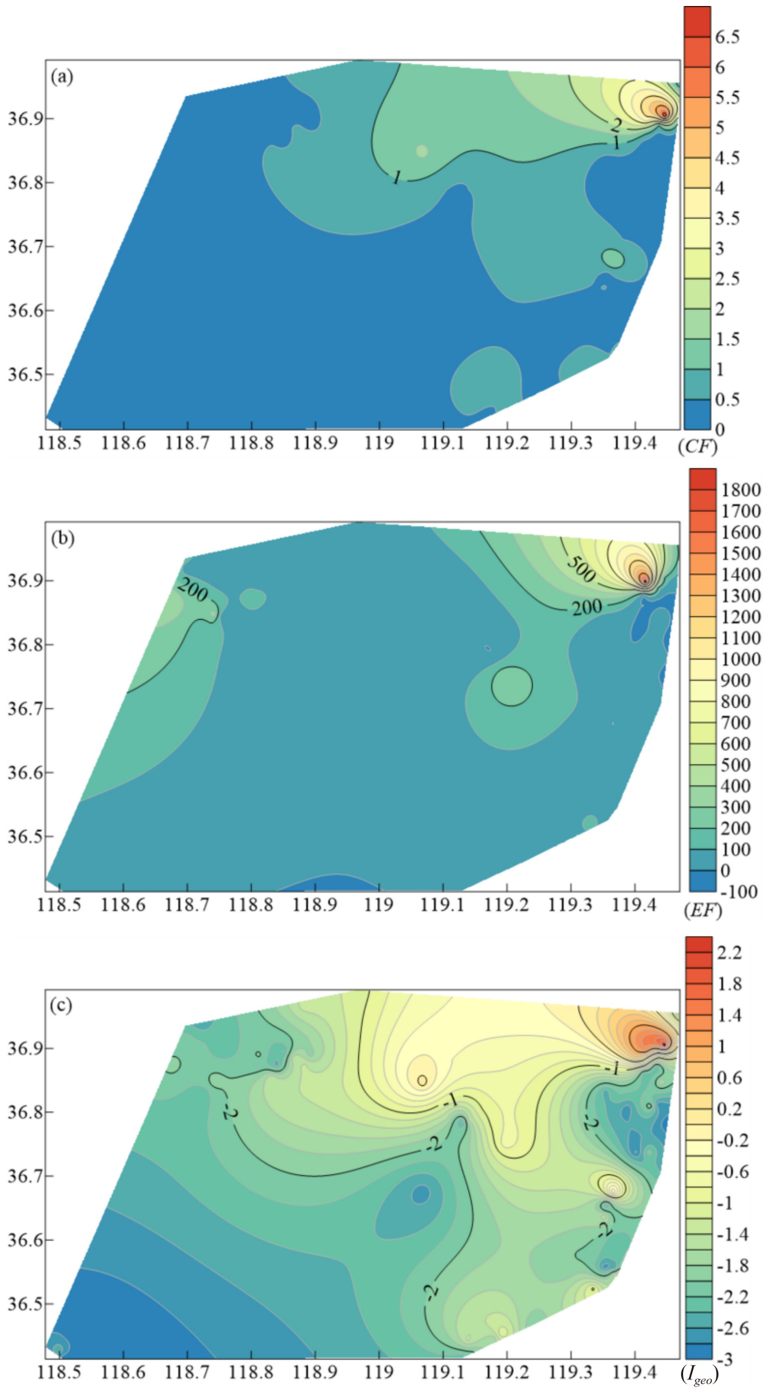

Fig. 10 Contamination assessment in dry season. (a) *CF*; (b) *EF*; (c) I_{geo}.

$$\frac{U}{ind(X)}=\left\{\begin{array}{l}\{SY1, SY5, SY12, SY57, SY58, SY65, SY69, SY70, SY83, SY89\}\\ \left\{\begin{array}{l}SY2, SY3, SY18, SY22, SY36, SY56, SY59, SY60, SY64, SY66, SY67, SY68, SY71, SY72\\ SY73, SY74, SY75, SY76, SY77, SY78, SY79, SY80, SY81, SY84, SY85, SY86, SY91, SY92\end{array}\right\}\\ \left\{\begin{array}{l}SY4, SY6, SY11, SY13, SY15, SY21, SY23, SY27, SY28, SY32, SY35, SY40, SY45, SY48, SY51\\ SY52, SY54, SY55, SY62, SY63, SY82, SY87, SY88, SY90\end{array}\right\}\\ \{SY7, SY16\},\quad \{SY8, SY24\}, \{SY9, SY19, SY29, SY33, SY38, SY42, SY49\}\\ \{SY10, SY14, SY26, SY34, SY39, SY41, SY43, SY44, SY46, SY47, SY50, SY53, SY61\}\\ \{SY17\}, \{SY20\}, \{SY25\},\quad \{SY30, SY31\}, \{SY37\}\end{array}\right\}$$

Table 4 Extension distance for SY01 in wet season and dry season

Indexes	Pollution degree											
	Level 1		Level 2		Level 3		Level 4		Level 5		Level 6	
	wet season	dry season	wet season	dry season	wet season	dry season	wet season	dry season	wet season	dry season	wet season	dry season
CF	0.065	−0.046	−0.065	0.108	0.170	0.417	0.524	0.880				
EF	0.999	0.013	0.998	0.012	0.995	0.011	0.979	0.002	0.959	−0.002	0.000	0.009
I_{geo}	0.019	−0.312	−0.019	1.100	0.381	1.574	0.781	2.048				

Taking *CF* as an example, the positive domain (*X*-*CF*) is given by:

$$pos_{X-X_1}(Q)=\left\{\begin{array}{l}\{SY1,SY10,SY12,SY13,SY14\},\ \{SY5\},\ \{SY6\},\ \{SY16,SY23\},\{SY22\}\\ \left\{\begin{array}{l}SY3,SY11,SY17,SY19,SY25,SY26,SY28,SY29,SY36,SY37,SY42\\ SY45,SY47,SY48,SY52,SY60,SY65,SY69,SY72,SY78,SY82,SY83,SY84\end{array}\right\}\\ \{SY21,SY24,SY27,SY30,SY32,SY33,SY34,SY38,SY40,SY41,SY43,SY44\}\\ \{SY20,SY31,SY35,SY39,SY46,SY81\}\end{array}\right\}\text{(wet season)}$$

$$pos_{X-X_1}(Q)=\left\{\begin{array}{l}\{SY7,SY16\},\ \{SY9,SY19,SY29,SY33,SY38,SY42,SY49\},\{SY17\},\ \{SY25\},\{SY30,SY31\}\\ \{SY10,SY14,SY26,SY34,SY39,SY41,SY43,SY44,SY46,SY47,SY50,SY53,SY61\}\end{array}\right\}\text{(dry season)}$$

The degree of dependence on *CF* is given by:

$$\gamma_{X-X_1}(Q)=\frac{\left|pos_{X-X_1}(Q)\right|}{|U|}=0.0920\,\text{(wet season)}$$

$$\gamma_{X-X_1}(Q)=\frac{\left|pos_{X-X_1}(Q)\right|}{|U|}=0.0652\,\text{(dry season)}$$

The importance of *CF* is given by:

$$\begin{aligned}\sigma_{XQ}(X_1)&=\gamma_X(Q)-\gamma_{X-X_1}(Q)\\&=1-\gamma_{X-X_1}(Q)=0.9080\,\text{(wet season)}\end{aligned}$$

$$\begin{aligned}\sigma_{XQ}(X_1)&=\gamma_X(Q)-\gamma_{X-X_1}(Q)\\&=1-\gamma_{X-X_1}(Q)=0.9348\,\text{(dry season)}\end{aligned}$$

EF and I_{geo} are similar, and the standardized weights are shown in Table 5.

It can be seen that the importance of these three indexes is *EF* > *CF*= I_{geo} in wet season, and in dry season *EF* > *CF*> I_{geo}.

Step 5: Identification of the close degree and pollution degree.

The close degree $N'_j(P_0)$ is calculated by

$$\begin{cases}D_{ji}=\left|V'_i-\dfrac{s_{ji}+t_{ji}}{2}\right|-\dfrac{t_{ji}-s_{ji}}{2}\\ N'_j(P_0)=1-\displaystyle\sum_{i=1}^{m}w_iD_{ji}\\ N'_j(P_0)=\max\left\{N'_j(P_0)\right\}\end{cases},$$

and the pollution degree caused by fluoride in groundwater during the wet and dry seasons in Mihe-Weihe River Basin, Shandong Peninsula is shown in Fig. 12.

Fig. 11 shows that the pollution degree is mainly Level 1 both in wet and dry seasons, accounting for 81.6% and 90.8%, followed by Level 6, accounting for 13.8% and 8.0%. In contrast to the dry season, 13.8% of the samples show a more severe fluoride pollution in wet season, in other words, the area of Level 6 expands, while that of Level 1 shrinks. It is speculated that the fluoride in fluorine-containing minerals is accelerated to be dissolved into the groundwater in wet season, causing groundwater quality deterioration in the Mihe-Weihe River Basin from dry season till wet season.

These samples, which are severely polluted by fluoride (Level 6), are mainly in the northern water source areas near Laizhou Bay, namely, Hanting, Changyi and Shouguang. It is speculated that there may be three reasons for this distribution: first, F-rich magmatic rocks and fluorine-containing minerals are widely distributed in the northeastern part of the Mihe-Weihe River Basin. By long-term weathering and leaching, a large amount of fluoride enters the groundwater. The second reason is that the terrain slopes gently in the northeastern part of the study area (interfluvial lowlands and alluvial-marine plains), and the groundwater runoff is slow, resulting in

Table 5 Standardized weights of indexes

Indexes	Season	σ_{XQ}	W_i
CF	Wet season	0.908	0.325
	Dry season	0.935	0.335
EF	Wet season	0.977	0.350
	Dry season	0.967	0.346
I_{geo}	Wet season	0.908	0.325
	Dry season	0.891	0.319

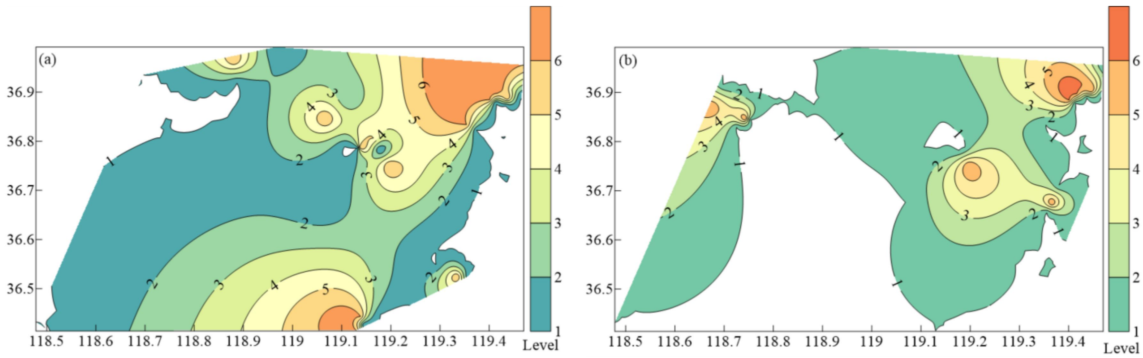

Fig. 11 (a) Pollution degree in wet season. (b) Pollution degree in dry season.

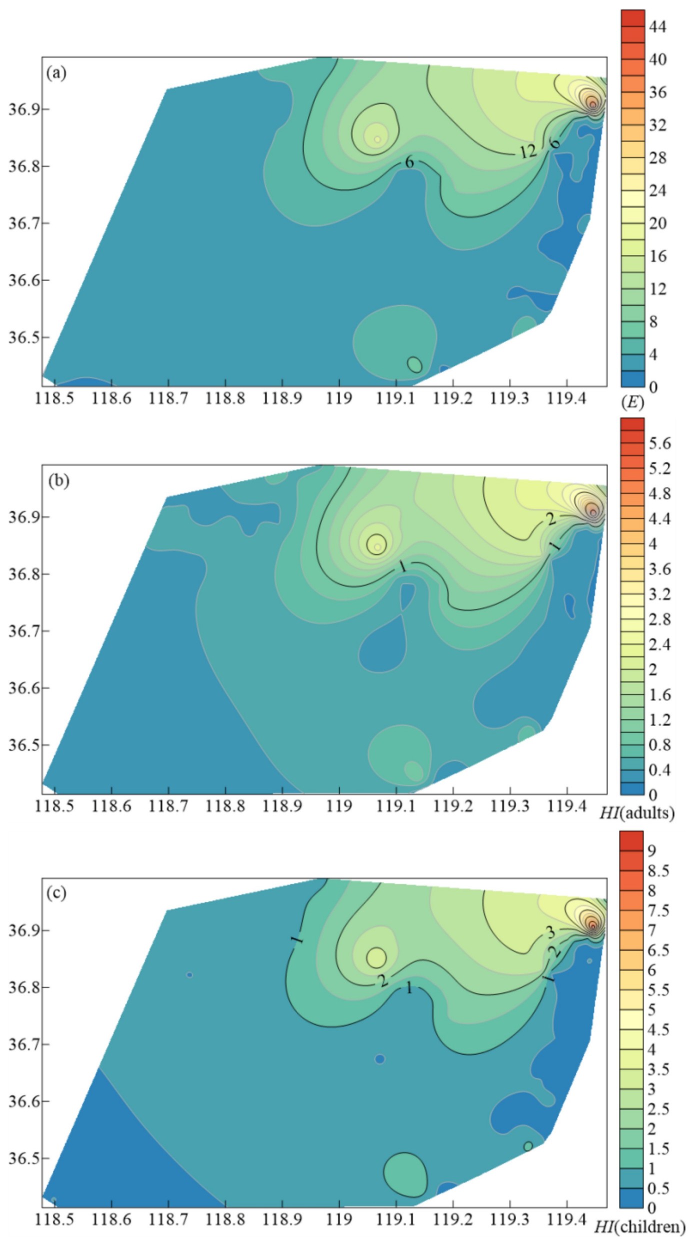

Fig. 12 Risk assessment in wet season. (a) *E*; (b) *HI* for adults; (c) *HI* for children.

the fluorine richness in shallow groundwater. Third one is, near Laizhou Bay, where human activities are frequent and intensive, it increases the pollution risks. In general, samples taken from the north are more severely polluted than those from the south. This may also be caused by groundwater flowing from southeast to northwest, it brings contaminants from upstream to downstream, and these contaminants accumulate in the downstream near Laizhou Bay. Therefore, it is necessary to focus on the groundwater quality in the northeast of Mihe-Weihe River Basin, especially in wet season, to reduce the ecological and health risks due to fluoride pollution, and the risks to human health caused by poor water quality should be paid attention to by the general public.

4.6.3 Ecological risk assessment

As shown in Figs. 12(a) and 13(a), almost all *E* values are less than 40 both in wet and dry seasons, only very few samples (Changyi water source area) show a moderate risk in wet season, and the potential ecological risks exist mainly in wet season.

4.6.4 Health risk assessment

As shown in Figs. 12(b) & 12(c) and 13(b) & 13(c), *HI* greater than 1 is mainly in the north, meaning more non-carcinogenic health risks for adults and children, and the risks in wet season are obviously stronger than dry season.

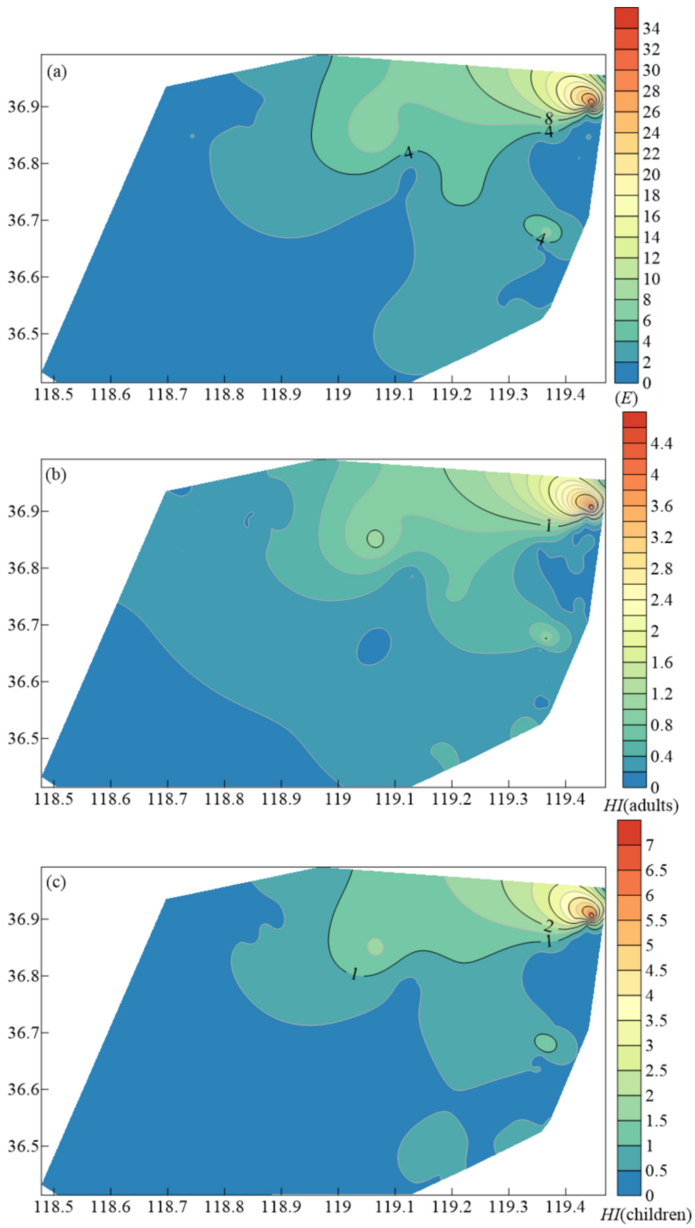

Fig. 13 Risk assessment in dry season. (a) *E*; (b) *HI* for adults; (c) *HI* for children.

5 Conclusions

1) Groundwater in the Mihe-Weihe River Basin is characterized by high TDS and weak alkalinity, and fluoride concentration in groundwater is generally on the high side, with a large area of medium-fluorine water (0.50 mg/L–1.00 mg/L). High-fluorine water is mainly in the northeast (interfluvial lowlands and alluvial-marine plains), which is HCO_3·Cl-Na- and HCO_3-Na-type water. In vertical direction, fluoride concentration decreases as the buried depth of groundwater level increases.

2) Fluorine richness in wet season is chiefly controlled by rock weathering and the dissolution of fluorine-containing minerals, and the weak alkaline environment, rich in sodium and poor in calcium, is the main reason for fluorine richness in dry season.

3) Contamination assessment results suggest that groundwater is severely polluted in the northeast of Mihe-Weihe River Basin, and wet season > dry season.

4) There are fewer ecological risks, but the health risks for adults and children should be paid attention to, especially in Weihan and Changyi water source areas during wet season.

Acknowledgements This work was supported by the Natural Science Foundation of Shandong Province (China) (Nos. ZR2020KE023 and ZR2021MD057) and the National Natural Science Foundation of China (No. 42002282).

Author Contributions Xingyue Qu: Conceptualization, Methodology, Software, Data curation, Writing-original draft. Peihe Zhai: Visualization, Investigation, Tests, Measurements and Analysis. Longqing Shi: Visualization, Investigation, Tests, Measurements and Analysis. Xingwei Qu: Supervision, Field investigation and Sampling. Ahmer Bilal: Software and Polishing. Jin Han and Xiaoge Yu: Software, Validation, Field investigation.

References

Andezhath S K, Susheela A K, Ghosh G (1999). Fluorosis management in India: the impact due to networking between health and rural drinking water supply agencies. IAHS-AISH Publication, 260: 159–165

Antoniadis V, Golia E E, Liu Y T, Wang S L, Shaheen S M, Rinklebe J (2019). Soil and maize contamination by trace elements and associated health risk assessment in the industrial area of Volos, Greece. Environment International, 124: 79–88

Ayoob S, Gupta A K (2006). Fluoride in drinking water: a review on the status and stress effects. Critical Reviews in Environmental Science and Technology, 36(6): 433–487

Cao Y Q, Bian Y J (2021). Improving the ecological environmental performance to achieve carbon neutrality: The application of DPSIR-improved matter-element extension cloud model. Journal of Environmental Management, 293: 112887

Chakravarty M, Patgiri A D (2009). Metal pollution assessment in sediments of the Dikrong River, NE India. Journal of Human Ecology (Delhi, India), 27(1): 63–67

Chen H Y, Teng Y G, Lu S J, Wang Y Y, Wang J S (2015). Contamination features and health risk of soil heavy metals in China. Science of the Total Environment, 512-513: 143-153 doi:10.1016/j.scitotenv.2015.01.025

Chernet T, Travi Y, Valles V (2001). Mechanism of degradation of the quality of natural water in the lakes region of the Ethiopian rift valley. Water Research, 35(12): 2819–2832

Dang P, Gu X, Lin C Y, Xin M, Zhang H, Ouyang W, Liu X T, He M C, Wang B D (2021). Distribution, sources, and ecological risks of potentially toxic elements in the Laizhou Bay, Bohai Sea: under the long-term impact of the yellow river input. Journal of Hazardous Materials, 413(3): 125429

Dehbandi R, Moore F, Keshavarzi B (2018). Geochemical sources, hydrogeochemical behavior, and health risk assessment of fluoride in an endemic fluorosis area, central Iran. Chemosphere, 193: 763–776

De Miguel E, Iribarren I, Chacon E, Ordonez A, Charlesworth S (2007). Risk-based evaluation of the exposure of children to trace elements in playgrounds in Madrid (Spain). Chemosphere, 66(3): 505–513

Du J Y, Wu D S, Xiao H Y, Li P (2011). Adsorption of fluoride on clay minerals and their mechanisms using X-ray photoelectron spectroscopy. Frontiers of Environmental Science & Engineering, 5(2): 212–226

Egli M, Mirabella A, Fitze P (2001). Clay mineral transformations in soils affected by fluorine and depletion of organic matter within a time span of 24 years. Geoderma, 103 (s3–4): 307–334

Gholizadeh M, Patimar R (2018). Ecological risk assessment of heavy metals in surface sediments from the Gorgan Bay, Caspian Sea. Marine Pollution Bulletin, 137: 662–667

Hakanson L (1980). An ecological risk index for aquatic pollution control, a sedimentological approach. Water Research, 14(8): 975–1001

Jacks G, Bhattacharya P, Chaudhary V, Singh K P (2005). Controls on the genesis of some high-fluoride groundwaters in India. Applied Geochemistry, 20(2): 221–228

Jayarathne T, Stockwell C E, Yokelson R J, Nakao S, Stone E A (2014). Emissions of fine particle fluoride from biomass burning. Environmental Science & Technology, 48(21): 12636–12644

Jia H F, Liang S D, Zhang Y S (2015). Assessing the impact on groundwater safety of inter-basin water transfer using a coupled modeling approach. Frontiers of Environmental Science & Engineering, 9(1): 84–95

Kharb P, Susheela A K (1994). Fluoride ingestion in excess and its effect on organic and certain inorganic constituents of soft tissues. Medical Science Research, 22: 43–44

Li X Q, Hou X W, Zhou Z C, Liu L X (2011). Geochemical provenance and spatial distribution of fluoride in groundwater of Taiyuan basin, China. Environmental Earth Sciences, 62(8): 1635–1642

Liaghati T, Preda M, Cox M (2004). Heavy metal distribution and controlling factors within coastal plain sediments, Bells Creek catchment, southeast Queensland, Australia. Environment International, 29(7): 935–948

Lin L Q (2009). Application of toxicological safety evaluation data to calculate Toxicity Coefficient of heavy metals. Beijing: Energy

Resources and Environment Professional Council of All-China Environment Federation, 60–63 (in Chinese)

Lv X L, Liu J T, Zhu L, Zhang Y X, Li H J (2020). Evolution feature and gensis of fluoride groundwater in shallow aquifer from Qin Wangchuan basin. Ganhanqu Ziyuan Yu Huanjing, 34(03): 188-195 (in Chinese)

Ma Z M, Mi J S, Lin Y T, Li J J (2022). Boundary region-based variable precision covering rough set models. Information Sciences, 608: 1524–1540

Mooreb D B, Levya D (2004). The shallow ground water chemistry of arsenic, fluorine, and major elements: Eastern Owens Lake, California. Applied Geochemistry, 14(1): 53–65

Muller G (1969). Index of geoaccumulation in sediments of the Rhine River. GeoJournal, 2: 108–118

Nielsen F H (2009). Micronutrients in parenteral nutrition: boron, silicon, and fluoride. Gastroenterology, 137(5): S55–S60

Pillai K S, Stanley V A (2002). Implications of fluoride-an endless uncertainty. Journal of Environmental Biology, 23: 81–87

Qiao J L, Cui Z M, Sun Y K, Hu Q H, Guan X H (2014). Simultaneous removal of arsenate and fluoride from water by Al-Fe (hydr)oxides. Frontiers of Environmental Science & Engineering, 8(2): 169–179

Reddy D V, Nagabhushanam P, Sukhija B S, Reddy A G S, Smedley P L (2010). Fluoride dynamics in the granitic aquifer of the Wailapally watershed, Nalgonda District, India. Chemical Geology, 269(3-4): 278-289 doi:10.1016/j.chemgeo.2009.10.003

Rinklebe J, Antoniadis V, Shaheen S M, Rosche O, Altermann M (2019). Health risk assessment of potentially toxic elements in soils along the Central Elbe River, Germany. Environment International, 126: 76–88

Sawassi A, Ottomano Palmisano G, Crookston B, Khadra R (2022). The dominance-based rough set approach for analysing patterns of flexibility allocation and design-cost criteria in large-scale irrigation systems. Agricultural Water Management, 272: 107842

USEPA (1989). Risk assessment guidance for Superfund human health evaluation manual (Part A). I. Office of Emergency and Remedial Response. Washington, DC: U.S. Environmental Protection Agency

USEPA (1993). Reference dose (RfD): description and use in health risk assessments. Background Document 1 A. Integrated Risk Information System (IRIS). Washington, DC: U.S. Environmental Protection Agency

USEPA (1997). Exposure factors handbook. Volume 1: General Factors. Washington, DC: U.S. Environmental Protection Agency, Office of Research and Development

USEPA (2002a). Child-specific exposure factors handbook. EPA-600-P-00-002B. Washington, DC: National Center for Environmental Assessment, U.S. Environmental Protection Agency

USEPA (2002b). Supplemental guidance for developing soil screening levels for Superfund sites. Washington, DC: U.S. Environmental Protection Agency

Wang Y L, Li F, Yang J L, Zhou M H, Song F H, Zhang D Y, Xue L, Zhu J R (2020). Demand response evaluation of RIES based on improved matter-element extension model. Energy, 212: 118121

World Health Organization (1993). Guidelines for drinking water quality, vol. I. Recommendations, 2nd edition. Geneva: WHO

Wu B, Zhao D Y, Jia H Y, Zhang Y, Zhang X X, Cheng S P (2009). Preliminary risk assessment of trace metal pollution in surface water from Yangtze River in Nanjing Section, China. Bulletin of Environmental Contamination and Toxicology, 82(4): 405–409

Xue W (2015). Statistical Analysis and the Applications of SPSS. Beijing: China Renmin University Press (in Chinese)

Yi Y J, Yang Z F, Zhang S H (2011). Ecological risk assessment of heavy metals in sediment and human health risk assessment of heavy metals in fishes in the middle and lower reaches of the Yangtze River basin. Environmental Pollution, 159(10): 2575–2585

Yin Z Y, Lin Q, Xu S H (2021). Using hydrochemical signatures to characterize the long-period evolution of groundwater information in the Dagu River Basin, China. Frontiers of Environmental Science & Engineering, 15(5): 105

Yu L, Zhang J J, Du C F, Yang H B, Ye B C (2018). Distribution and pollution evaluation of fluoride in a soil-water-plant system in Shihezi, Xinjiang, China. Human and Ecological Risk Assessment, 24(2): 445–455

Zhang Y, Peng Z, Dong Z M, Wang M J, Jiang C (2022). Twenty years of achievements in China's implementation of the Stockholm Convention. Frontiers of Environmental Science & Engineering, 16(12): 152